THE GEOLOGICAL SOCIETY OF AMERICA®

Compositional transition in natural alkaline lavas through silica-undersaturated melt–lithosphere interaction

Ze-Zhou Wang[1], Sheng-Ao Liu[1]*, Li-Hui Chen[2], Shu-Guang Li[1, 3], and Gang Zeng[2]
[1]State Key Laboratory of Geological Processes and Mineral Resources, China University of Geosciences, Beijing 100083, China
[2]State Key Laboratory for Mineral Deposits Research, School of Earth Sciences and Engineering, Nanjing University, Nanjing 210093, China
[3]Chinese Academy of Sciences Key Laboratory of Crust-Mantle Materials and Environments, University of Science and Technology of China, Hefei, Anhui 230026, China

ABSTRACT

Natural alkaline lavas have diverse compositions—varying widely from nephelinite through basanite to alkali olivine basalt—the origin of which is controversial. In particular, identifying the roles of recycling carbonates in the source and evolution of natural alkaline lavas is commonly difficult. Zinc isotope ratios (δ^{66}Zn) have great potential due to the strong δ^{66}Zn contrast between marine carbonates and the mantle. Here we present a systematic variation of Zn isotopes with Sr-Nd isotopes and incompatible elements (e.g., Nb, Th, and Zn) in nephelinites, basanites, and alkali olivine basalts from eastern China. The elevated δ^{66}Zn of nephelinites and high-alkali basanites relative to the mantle demonstrates that the silica-undersaturated melts were derived from a carbonated mantle. Alkali olivine basalts and low-alkali basanites show a gradual decline of δ^{66}Zn with SiO_2 and have Zn-Sr-Nd isotopic and chemical compositions shifted toward that of an enriched lithospheric mantle. Infiltration of silica-undersaturated basanitic melts and reaction with the lithospheric mantle account for the transition of strongly alkaline melts into weakly alkaline melts via consumption of orthopyroxene and mixing with silica-rich melt derived from lithospheric mantle. High-δ^{66}Zn wehrlite xenoliths found in these alkaline lavas record metasomatism of the lithospheric mantle by basanitic melts. Thus, silica-undersaturated melt–lithosphere interaction could be one of the most common causes of compositional diversity in natural alkaline lavas.

INTRODUCTION

Intraplate alkaline lavas are typically silica-undersaturated and alkali-rich relative to tholeiitic or calc-alkaline lavas erupted at plate boundaries. Their unique chemical and isotope signatures manifest the compositional heterogeneities of Earth's mantle, associated with recycling of crust materials (e.g., Hofmann, 1997). Natural alkaline lavas commonly exhibit a wide range of chemical compositions, from nephelinite through basanite to alkali olivine basalt, with a respective increase in silica and a decrease in alkalinity. The origin of this compositional transition, observed in intraplate volcanoes, is fundamental in petrology and has long been debated.

Trace element modeling indicates that increasing degree of melting of garnet peridotite or fractional crystallization facilitates the transition from nephelinite to alkali olivine basalt (e.g., O'Hara and Yoder, 1967; Frey et al., 1978; Caroff et al., 1997). However, experimental results show that natural alkaline lavas can hardly be produced by melting of volatile-free peridotite (Kogiso et al., 2003). As a possible resolution, melting of CO_2- or carbonate-bearing peridotites has reproduced a series of liquids that overlap part of the natural trend (Hirose, 1997; Dasgupta et al., 2007). Nevertheless, the melting degrees (5%–33%) obtained in experiments (e.g., Dasgupta et al., 2007) are too high to match those (1%–8%) calculated on the basis of trace elements (e.g., Caroff et al., 1997). An alternative mechanism for the nephelinite–alkali basalt transition is reaction of silica-undersaturated melt with subsolidus peridotite, during which melts are diluted by the progressive dissolution of orthopyroxene leading to an enrichment of silica and a decrease of alkalis and incompatible trace elements (Lundstrom, 2000; Pilet et al., 2008; Zhang et al., 2017; Li and Wang, 2018). Discriminating the above hypotheses requires an effective tool to distinguish a carbonated source from other sources (e.g., hybridization by recycled siliciclastic sediments), which is commonly difficult using traditional isotope approaches (e.g., Sr, Pb, and O isotopes). Zinc stable isotopes have such a potential owing to the remarkable δ^{66}Zn difference, but the same orders of magnitude of Zn concentrations between silicate reservoirs (mantle, oceanic mafic crust, and siliciclastic sediments; δ^{66}Zn = ~0.2‰–0.3‰) and marine carbonates (average δ^{66}Zn = ~0.91‰) (Fig. DR1 in the GSA Data Repository[1]; Liu et al., 2016).

Cenozoic alkaline basaltic lavas in the Shandong Peninsula of eastern China encompass a broad range of compositions from nephelinite through basanite to alkali olivine basalt, and are regarded as one of classic examples for studying the origin of intraplate alkaline lavas (Sakuyama et al., 2013; Zeng et al., 2010; H.-Y. Li et al., 2017; S.-G. Li et al., 2017). Here we report new Zn isotope data and compile available Sr-Nd isotope and major-trace element data on these alkaline lavas. These results shed light on the important role of interaction of carbonated mantle-derived silica-undersaturated melt with the overlying lithosphere in generating the compositional diversity of intraplate alkaline lavas.

GEOLOGICAL BACKGROUND AND SAMPLES

Alkaline basaltic lavas have been emplaced over a distance of >4000 km from north to south in eastern China since ca. 106 Ma, constituting an important part of the western circum-Pacific volcanic belt (Fig. DR2). Seismic tomography has revealed that subducting Pacific slabs are stagnant in the mantle transition zone (MTZ) beneath eastern China (Fukao et al., 1992). These basalts have chemical and radiogenic isotopic compositions comparable to those of ocean island basalts (OIBs) and represent typical intraplate alkaline lavas derived from an asthenospheric source (e.g., Zhou and Armstrong, 1982; S.-G. Li et al., 2017), which is probably located above the MTZ (S.-G. Li et al., 2017). A total of 57 representative samples from Shandong Peninsula were selected for this study. Their eruption lasted from 24.0 to 0.3 Ma,

*E-mail: lsa@cugb.edu.cn

[1]GSA Data Repository item 2018280, analytical methods, modeling details, Figures DR1–DR5, and Table DR1, is available online at http://www.geosociety.org/datarepository/2018/ or on request from editing@geosociety.org.

with alkali olivine basalt at the early stage and nephelinite at the late stage (Zeng et al., 2010). The presence of abundant mantle xenoliths reflects rapid emplacement of the host lavas. All samples have minor olivine as phenocrysts set in a groundmass of olivine, Ti-magnetite, nepheline, and glass, but are devoid of plagioclase and pyroxene phenocrysts. Petrology and geochemistry of these samples have been well characterized (Zeng et al., 2010, 2011).

RESULTS

Zinc isotope data are available in Table DR1 in the Data Repository, together with data for selected elements and Sr-Nd isotopes. The overall range of δ^{66}Zn is from 0.31‰ to 0.48‰, greatly exceeding the range of the upper mantle (0.20‰ ± 0.05‰; 2σ) and mid-oceanic ridge basalts (MORBs) (0.28‰ ± 0.03‰; 2σ) (Wang et al., 2017). Nephelinites (0.45‰ ± 0.04‰; 2σ) have higher δ^{66}Zn than alkali olivine basalts (0.34‰ ± 0.06‰; 2σ), the latter of which has values that lie between those of nephelinites and MORBs. Alkali olivine basalts show a striking δ^{66}Zn decline with increasing SiO_2 and decreasing alkalis and incompatible elements such as Nb, Th, and Zn, whereas nephelinites do not (Figs. 1 and 2). The δ^{66}Zn values of high-alkali basanites overlap those of nephelinites, but some low-alkali basanites have δ^{66}Zn values within the range of alkali olivine basalts.

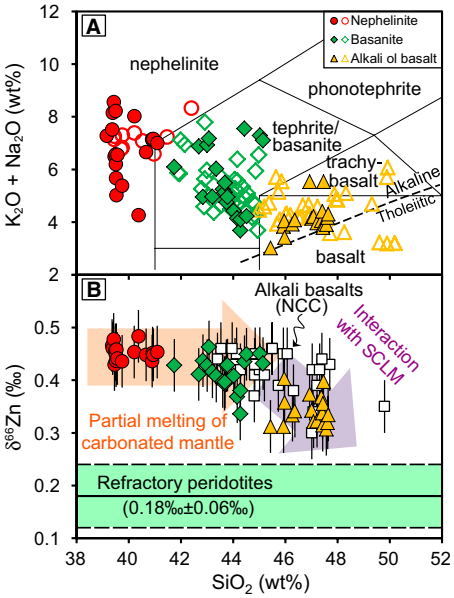

Figure 1. A: Total alkali versus SiO_2 diagram for classification of alkaline lavas from Shandong Peninsula, eastern China. Solid symbols denote samples in this study; open symbols represent literature data (see data sources in Fig. DR5 [see footnote 1]). B: Plot of δ^{66}Zn versus SiO_2. Error bars represent 2σ. Data for alkali basalts from the North China craton (NCC) and refractory peridotites are from Liu et al. (2016) and Wang et al. (2017), respectively. ol—olivine; SCLM—sub-continental lithospheric mantle.

ORIGIN OF STRONGLY ALKALINE BASALTS

The lack of correlation of δ^{66}Zn with loss on ignition, MgO, Cr, and Ni (Fig. DR3) indicates that secondary alteration, crustal contamination, and fractional crystallization negligibly affect Zn isotopes. Primary melts from a volatile-free peridotite source have δ^{66}Zn <0.3‰ (Wang et al., 2017), and thus the elevated δ^{66}Zn must reflect mantle hybridization by ^{66}Zn-enriched agents. Trace element characteristics (e.g., high Ce/Pb and U/Pb, low Ba/Th and Rb/Nb; Figs. 2E and 2F; Fig. DR4) suggest that the nephelinite and high-alkali basanites have a strong high-μ (HIMU) affinity (high $^{238}U/^{204}Pb$), indicating a source dominated by dehydrated oceanic crust (e.g., Hofmann, 1997; Kogiso et al., 1997; Willbold and Stracke, 2006), probably together with subducted carbonates (Castillo, 2015). Because dehydrated oceanic crust has

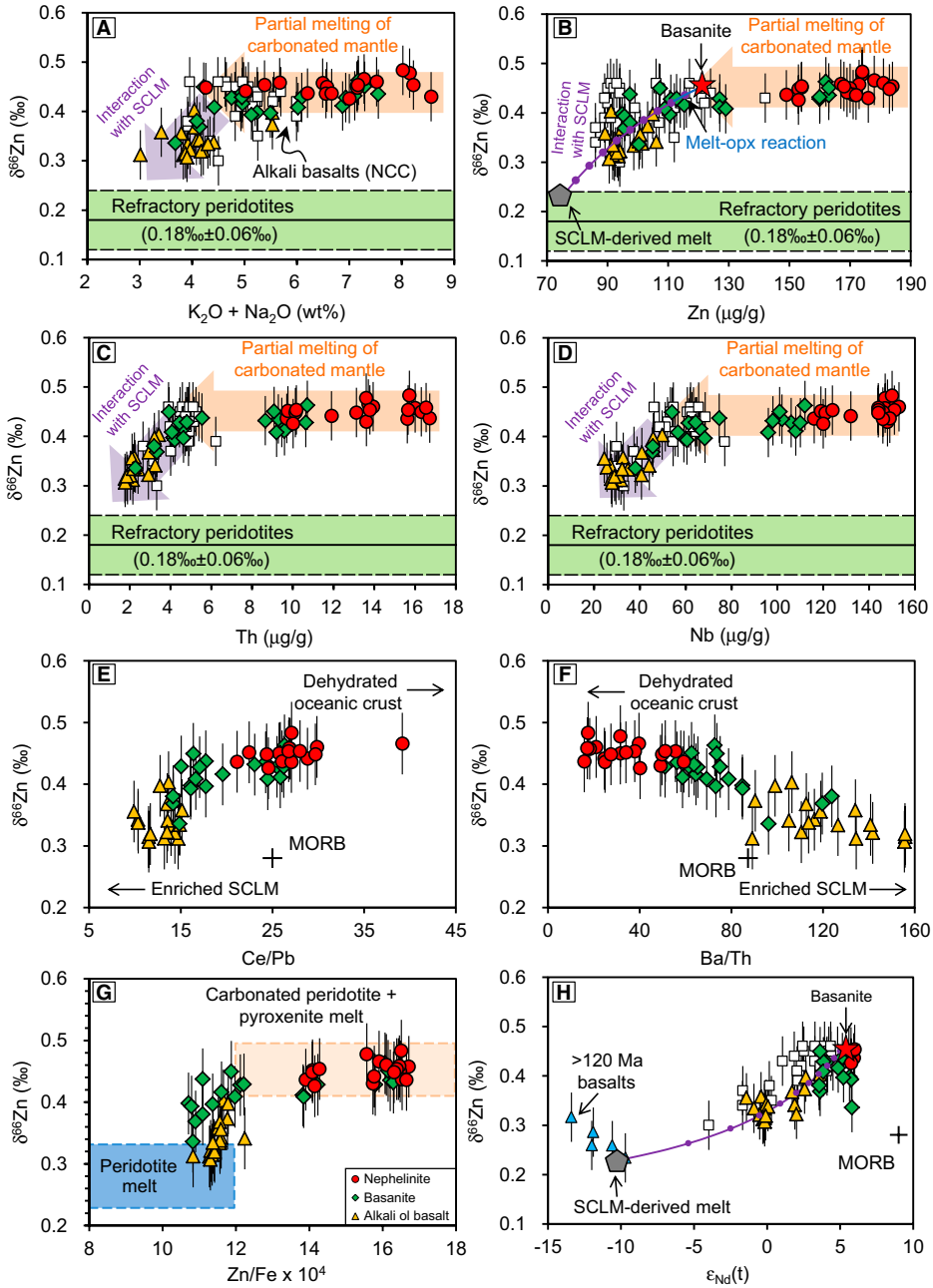

Figure 2. Variations of δ^{66}Zn with $K_2O + Na_2O$ (A), Zn (B), Th (C), Nb (D), Ce/Pb (E), Ba/Th (F), Zn/Fe (G), and $\varepsilon_{Nd}(t)$ (H). Error bars represent 2σ. Data for alkali basalts and >120 Ma basalts from North China craton (NCC) are from Liu et al. (2016). δ^{66}Zn of refractory peridotite and mid-oceanic ridge basalt (MORB) are from Wang et al. (2017). The Zn/Fe ranges of peridotite and pyroxenite melts are from Le Roux et al. (2010). Solid curves in B and H represent evolution of basanite during reaction with orthopyroxene (opx) (blue) or mixing with sub-continental lithospheric mantle (SCLM)–derived melt (purple). Increment of mixing curves (small dot) is 0.1. Details of calculations are shown in the Data Repository (see footnote 1).

slightly lower δ^{66}Zn relative to MORBs due to preferential release of ^{66}Zn-enriched fluids during slab dehydration (Pons et al., 2016), marine carbonates are the unique candidate for the ^{66}Zn-enriched agents. Even if carbonate is a minor phase of oceanic crust, deep subducted (ultrahigh-pressure) carbonate species (e.g., magnesite) could have very high Zn concentration (up to ~450 µg/g; Li et al., 2014) relative to the upper mantle (~55 µg/g; Le Roux et al., 2010). Mixing of ~4.4% carbonates with the mantle can result in an elevated δ^{66}Zn of up to 0.45‰. Thereupon, melting of carbonate-bearing dehydrated oceanic crust accounts for the high-δ^{66}Zn mantle source for strongly alkaline lavas.

TRANSITION FROM BASANITE TO WEAKLY ALKALINE BASALTS

The covariations of δ^{66}Zn with Nd isotopes and key elements can be separated into two distinct trends (Figs. 1 and 2). One trend is defined by nephelinites and high-alkali basanites that have variable concentrations of incompatible elements but uniform δ^{66}Zn, reflecting the modest Zn isotope fractionation during mantle melting (Wang et al., 2017). Trace element modeling suggests 1.5%–4% melting in the garnet stability field (Zeng et al., 2010). Another trend is defined by alkali olivine basalts and low-alkali basanites that show covariations of δ^{66}Zn with $\varepsilon_{Nd}(t)$ and incompatible elements. Because isotopic ratios are almost unfractionated during equilibrium melting, this trend demands mixing/interaction of two chemically and isotopically distinct sources. Extrapolation of these trendlines (Fig. 2) separates the two sources into basanite and an enriched mantle component, respectively.

Recycled ancient eclogite and garnet pyroxenite were previously presumed to be the enriched component in the mantle (Zeng et al., 2011; H.-Y. Li et al., 2017). However, the alkali olivine basalts and low-alkali basanites have low Zn/Fe ratios typical of a peridotitic rather than a pyroxenitic source lithology (Fig. 2G). The enriched component is most likely the subcontinental lithospheric mantle (SCLM) modified by slab-derived fluids and/or melts as indicated by the high Ba/Th and low Ce/Pb of alkali olivine basalts and low-alkali basanites (Figs. 2E and 2F). Although most peridotite xenoliths entrained in these alkaline lavas have low ^{87}Sr/^{86}Sr and high $\varepsilon_{Nd}(t)$, they sampled the shallow SCLM that is located above and thus may differ in composition from the source region of alkali olivine basalts capturing the xenoliths. In fact, peridotite xenoliths with extremely enriched Sr-Nd isotope compositions are widely found in mafic intrusions from Shandong Peninsula (Fig. 3; Fig. DR5). These "enriched" peridotites also contain high abundances of fluid-mobile elements like Ba and Pb (Xu et al., 2008) and have low La/Yb ratios (Fig. 3). Highly enriched mantle signals [e.g., low $\varepsilon_{Nd}(t)$] are also recorded

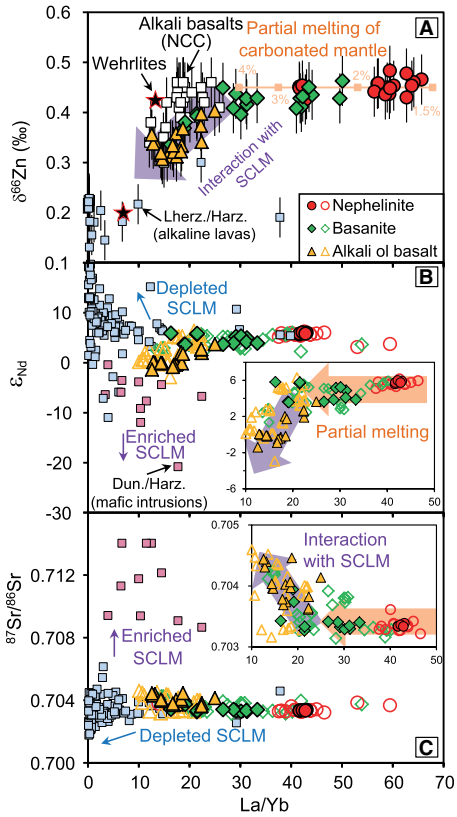

Figure 3. Variations of La/Yb ratios with isotopic ratios of Zn (A), Nd (B), and Sr (C). δ^{66}Zn of wehrlite, lherzolite (Lherz.), and harzburgite (Harz.) are from Wang et al. (2017), and ^{87}Sr/^{86}Sr, ε_{Nd}, and La/Yb are compiled from literature (see the Data Repository [see footnote 1]). Error bars represent 2σ. Orange line refers to degree of partial melting as function of La/Yb (after Zeng et al., 2010). NCC—North China craton; SCLM—sub-continental lithospheric mantle; Dun.—dunite.

in the SCLM-derived lavas (>120 Ma basalts; Fig. 2H). These lines of evidence suggest that substantial reaction of basanitic melts with an enriched SCLM is highly probable. The existence of high-δ^{66}Zn wehrlite xenoliths is the direct record of metasomatism of the SCLM by ^{66}Zn-rich basanitic melts (Fig. 3A).

Considerable CO_2 can be dissolved in primary melts of basanite and nephelinite (Dasgupta et al., 2007), but reaction of CO_2-rich basanitic melts with peridotite would dissolve olivine and produce strongly silica-undersaturated melilitite instead of less silica-undersaturated melts (Mallik and Dasgupta, 2013). In fact, the primary basanitic melts derived from melting of carbonated mantle could have undergone extensive degassing in the upper mantle (1–4 GPa) (Boudoire et al., 2018). Degassing may also be enhanced along deep faults such as the Tan-Lu fault where weakly alkaline basalts erupted (Fig. DR2) during continental rifting (Lee et al., 2016). Subsequently, reactive infiltration of the CO_2-poor silica-undersaturated melt into the SCLM would gradually transform silica-undersaturated melts into less silica-undersaturated ones via olivine crystallization at the expense of orthopyroxene (Shaw et al., 1998; Lundstrom, 2000; Pilet et al., 2008), with a concomitant decrease in incompatible elements and δ^{66}Zn by dilution (Figs. 1 and 2). However, reaction of melts with orthopyroxene alone cannot generate the δ^{66}Zn-[Zn] trend in alkali olivine basalts (Fig. 2B), as orthopyroxene is too poor in Zn. Lundstrom (2000) found that infiltration of sodium into peridotite not only causes dissolution of orthopyroxene but can also change the manner by which the peridotite melts by a process that is chemically, not thermally, activated. Hence, silica-rich melts with lower δ^{66}Zn and La/Yb ratios than the basanite can be produced by melting of SLCM at shallow depth during basanite-peridotite interaction. A binary mixing model suggests that mixing of the percolated basanite with ~30% to 70% of SCLM melt is able to reproduce the δ^{66}Zn-[Zn] and δ^{66}Zn-$\varepsilon_{Nd}(t)$ trends observed in the alkali olivine basalts (Figs. 2B and 2H). Such amounts of SCLM melts can be generated near the interface between basanitic melt and impregnated peridotite (Lundstrom, 2000).

COMPOSITIONAL DIVERSITY IN INTRAPLATE ALKALINE LAVAS

The compositional continuum from nephelinites to alkali olivine basalts observed in many other intraplate alkaline lava suites (e.g., Hawaii, southeastern Australia, and Tubuai [French Polynesia]) has been commonly attributed to increasing degrees of mantle melting (e.g., Frey et al., 1978; Clague and Frey, 1982; Caroff et al., 1997). However, systematic isotopic variations found in some alkaline lavas from a geographically and temporally limited volcanic province indicate multiple sources (e.g., Zhang et al., 2017). Our study supports the experimental results showing that melting of a carbonated mantle can only generate the nephelinite-basanite series (Hirose, 1997; Dasgupta et al., 2007), whereas reaction of silica-undersaturated basanitic melts with lithosphere is required for a complete transition from basanite into alkali olivine basalts and even tholeiites (Pilet et al., 2008). The composition of alkaline lavas could be efficiently modified when they ascend through the overlying lithosphere. Such processes are perhaps frequently identified where the lithospheric mantle is isotopically distinct from the percolated melts. It is interesting that strongly silica-undersaturated lavas (e.g., nephelinite) commonly occur later than alkali olivine basalts and tholeiites from the same area (e.g., eastern China, Hawaii). The temporal sequence may reflect transition of the incipient strongly alkaline melts to weakly alkaline melts via interaction with the SCLM. Silica-undersaturated melt–peridotite interaction could be one of the key processes responsible for the compositional diversity that is ubiquitously

observed in natural alkaline magmatism (Pilet et al., 2008).

ACKNOWLEDGMENTS

We are grateful to three anonymous reviewers for their constructive comments and to editor Chris Clark for his careful editorial handling. This work is supported by the Strategic Priority Research Program (B) of the Chinese Academy of Sciences (grant XDB18000000) and the National Natural Science Foundation of China (grants 41622303 and 41730214).

REFERENCES CITED

Boudoire, G., Rizzo, A.L., Di Muro, A., Grassa, F., and Liuzzo, M., 2018, Extensive CO_2 degassing in the upper mantle beneath oceanic basaltic volcanoes: First insights from Piton de la Fournaise volcano (La Réunion Island): Geochimica et Cosmochimica Acta, v. 235, p. 376–401, https://doi.org/10.1016/j.gca.2018.06.004.

Caroff, M., Maury, R.C., Guille, G., and Cotten, J., 1997, Partial melting below Tubuai (Austral Islands, French Polynesia): Contributions to Mineralogy and Petrology, v. 127, p. 369–382, https://doi.org/10.1007/s004100050286.

Castillo, P.R., 2015, The recycling of marine carbonates and sources of HIMU and FOZO ocean island basalts: Lithos, v. 216–217, p. 254–263, https://doi.org/10.1016/j.lithos.2014.12.005.

Clague, D.A., and Frey, F.A., 1982, Petrology and trace element geochemistry of the Honolulu Volcanics, Oahu: Implications for the oceanic mantle below Hawaii: Journal of Petrology, v. 23, p. 447–504, https://doi.org/10.1093/petrology/23.3.447.

Dasgupta, R., Hirschmann, M.M., and Smith, N.D., 2007, Partial melting experiments of peridotite + CO_2 at 3 GPa and genesis of alkalic ocean island basalts: Journal of Petrology, v. 48, p. 2093–2124, https://doi.org/10.1093/petrology/egm053.

Frey, F.A., Green, D.H., and Roy, S.D., 1978, Integrated models of basalt petrogenesis: A study of quartz tholeiites to olivine melilitites from south eastern Australia utilizing geochemical and experimental petrological data: Journal of Petrology, v. 19, p. 463–513, https://doi.org/10.1093/petrology/19.3.463.

Fukao, Y., Obayashi, M., Inoue, H., and Nenbai, M., 1992, Subducting slabs stagnant in the mantle transition zone: Journal of Geophysical Research, v. 97, p. 4809–4822, https://doi.org/10.1029/91JB02749.

Hirose, K., 1997, Partial melt compositions of carbonated peridotite at 3 GPa and role of CO_2 in alkali-basalt magma generation: Geophysical Research Letters, v. 24, p. 2837–2840, https://doi.org/10.1029/97GL02956.

Hofmann, A.W., 1997, Mantle geochemistry: The message from oceanic volcanism: Nature, v. 385, p. 219–229, https://doi.org/10.1038/385219a0.

Kogiso, T., Tatsumi, Y., and Nakano, S., 1997, Trace element transport during dehydration processes in the subducted oceanic crust: 1. Experiments and implications for the origin of ocean island basalts: Earth and Planetary Science Letters, v. 148, p. 193–205, https://doi.org/10.1016/S0012-821X(97)00018-6.

Kogiso, T., Hirschmann, M.M., and Frost, D.J., 2003, High-pressure partial melting of garnet pyroxenite: Possible mafic lithologies in the source of ocean island basalts: Earth and Planetary Science Letters, v. 216, p. 603–617, https://doi.org/10.1016/S0012-821X(03)00538-7.

Lee, H., Muirhead, J.D., Fischer, T.P., Ebinger, C.J., Kattenhorn, S.A., Sharp, Z.D., and Kianji, G., 2016, Massive and prolonged deep carbon emissions associated with continental rifting: Nature Geoscience, v. 9, p. 145–149, https://doi.org/10.1038/ngeo2622.

Le Roux, V., Lee, C.-T.A., and Turner, S.J., 2010, Zn/Fe systematics in mafic and ultramafic systems: Implications for detecting major element heterogeneities in the Earth's mantle: Geochimica et Cosmochimica Acta, v. 74, p. 2779–2796, https://doi.org/10.1016/j.gca.2010.02.004.

Li, H.-Y., Xu, Y.-G., Ryan, J.G., and Whattam, S.A., 2017, Evolution of the mantle beneath the eastern North China Craton during the Cenozoic: Linking geochemical and geophysical observations: Journal of Geophysical Research: Solid Earth, v. 122, p. 224–246, https://doi.org/10.1002/2016JB013486.

Li, J.-L., Klemd, R., Gao, J., and Meyer, M., 2014, Compositional zoning in dolomite from lawsonite-bearing eclogite (SW Tianshan, China): Evidence for prograde metamorphism during subduction of oceanic crust: The American Mineralogist, v. 99, p. 206–217, https://doi.org/10.2138/am.2014.4507.

Li, S.-G., and Wang, Y., 2018, Formation time of the big mantle wedge beneath eastern China and a new lithospheric thinning mechanism of the North China craton—Geodynamic effects of deep recycled carbon: Science China: Earth Sciences, https://doi.org/10.1007/s11430-017-9217-7 (in press).

Li, S.-G., et al., 2017, Deep carbon cycles constrained by a large-scale mantle Mg isotope anomaly in eastern China: National Science Review, v. 4, p. 111–120, https://doi.org/10.1093/nsr/nww070.

Liu, S.-A., Wang, Z.-Z., Li, S.-G., Huang, J., and Yang, W., 2016, Zinc isotope evidence for a large-scale carbonated mantle beneath eastern China: Earth and Planetary Science Letters, v. 444, p. 169–178, https://doi.org/10.1016/j.epsl.2016.03.051.

Lundstrom, C.C., 2000, Rapid diffusive infiltration of sodium into partially molten peridotite: Nature, v. 403, p. 527–530, https://doi.org/10.1038/35000546.

Mallik, A., and Dasgupta, R., 2013, Reactive infiltration of MORB-eclogite-derived carbonated silicate melt into fertile peridotite at 3 GPa and genesis of alkalic magmas: Journal of Petrology, v. 54, p. 2267–2300, https://doi.org/10.1093/petrology/egt047.

O'Hara, M.J., and Yoder, H.S., 1967, Formation and fractionation of basic magmas at high pressures: Scottish Journal of Geology, v. 3, p. 67–117, https://doi.org/10.1144/sjg03010067.

Pilet, S., Baker, M.B., and Stolper, E.M., 2008, Metasomatized lithosphere and the origin of alkaline lavas: Science, v. 320, p. 916–919, https://doi.org/10.1126/science.1156563.

Pons, M.-L., Debret, B., Bouilhol, P., Delacour, A., and Williams, H., 2016, Zinc isotope evidence for sulfate-rich fluid transfer across subduction zones: Nature Communications, v. 7, 13794, https://doi.org/10.1038/ncomms13794.

Sakuyama, T., et al., 2013, Melting of dehydrated oceanic crust from the stagnant slab and of the hydrated mantle transition zone: Constraints from Cenozoic alkaline basalts in eastern China: Chemical Geology, v. 359 p.32–48, https://doi.org/10.1016/j.chemgeo.2013.09.012.

Shaw, C.S., Thibault, Y., Edgar, A.D., and Lloyd, F.E., 1998, Mechanisms of orthopyroxene dissolution in silica-undersaturated melts at 1 atmosphere and implications for the origin of silica-rich glass in mantle xenoliths: Contributions to Mineralogy and Petrology, v. 132, p. 354–370, https://doi.org/10.1007/s004100050429.

Wang, Z.-Z., Liu, S.-A., Liu, J., Huang, J., Xiao, Y., Chu, Z.-Y., Zhao, X.-M., and Tang, L., 2017, Zinc isotope fractionation during mantle melting and constraints on the Zn isotope composition of Earth's upper mantle: Geochimica et Cosmochimica Acta, v. 198, p. 151–167, https://doi.org/10.1016/j.gca.2016.11.014.

Willbold, M., and Stracke, A., 2006, Trace element composition of mantle end-members: Implications for recycling of oceanic and upper and lower continental crust: Geochemistry Geophysics Geosystems, v. 7, Q04004, https://doi.org/10.1029/2005GC001005.

Xu, W., Hergt, J.M., Gao, S., Pei, F., Wang, W., and Yang, D., 2008, Interaction of adakitic melt-peridotite: Implications for the high-Mg# signature of Mesozoic adakitic rocks in the eastern North China Craton: Earth and Planetary Science Letters, v. 265, p. 123–137, https://doi.org/10.1016/j.epsl.2007.09.041.

Zeng, G., Chen, L.-H., Xu, X.-S., Jiang, S.-Y., and Hofmann, A.W., 2010, Carbonated mantle sources for Cenozoic intra-plate alkaline basalts in Shandong, North China: Chemical Geology, v. 273, p. 35–45, https://doi.org/10.1016/j.chemgeo.2010.02.009.

Zeng, G., Chen, L.-H., Hofmann, A.W., Jiang, S.-Y., and Xu, X.-S., 2011, Crust recycling in the sources of two parallel volcanic chains in Shandong, North China: Earth and Planetary Science Letters, v. 302, p. 359–368, https://doi.org/10.1016/j.epsl.2010.12.026.

Zhang, G.-L., Chen, L.-H., Jackson, M.G., and Hofmann, A.W., 2017, Evolution of carbonated melt to alkali basalt in the South China Sea: Nature Geoscience, v. 10, p. 229–235, https://doi.org/10.1038/ngeo2877.

Zhou, X., and Armstrong, R.L., 1982, Cenozoic volcanic rocks of eastern China—Secular and geographic trends in chemistry and strontium isotopic composition: Earth and Planetary Science Letters, v. 58, p. 301–329, https://doi.org/10.1016/0012-821X(82)90083-8.

Manuscript received 11 May 2018
Revised manuscript received 28 June 2018
Manuscript accepted 6 July 2018

Printed in USA